Numerical Fault Arc Simulation Based on Power Arc Tests

M. Kizilcay, K.-H. Koch

Abstract

More than 200 power arc tests were carried out with original arrangements of overhead line insulators and arcing fittings for 20 kV, 110 kV and 220 kV. With an adequately modelled network, short-circuit currents in the range of 2 kA to 12.5 kA can be realized. Analysis of the measurements shows that a typical arc voltage time function can be attributed to each insulator type and arrangement. Using the measured variables, which were digitally recorded and stored on optical media, an existing numerical arc model has been enhanced, which can be applied in an electromagnetic transients program to reproduce the dynamic and random behaviour of power arcs for any insulator arrangement, current and system voltage.

1 Introduction

In the case of short-circuits occurring on lines within medium- and high-voltage networks the distance protection has to locate precisely the fault point for a selective interruption of the faulty line. The exact distance of the fault point is measured by evaluating the impedance resulting from line voltage and line current at the beginning of the line. In most cases, however, short circuits in a network are power fault arcs so that an impedance evaluation is disturbed by the arc voltage arising at the fault point. The fault arc has not only a non-linear current/voltage characteristic but also is its length time-varying due to forces acting on it. Electrodynamical force, thermal buoyancy and wind cause the arc to elongate between its roots or to move along the line conductor with one of its roots. Abrupt changes in the arc voltage are caused by a breakdown between arc sections.

The arc voltage also depends on how the insulators for overhead lines and the arcing fittings are arranged. It also depends on how much space is disposable, i. e. whether the space is unlimited or limited by insulating material as is in the case of cables. If the space is unlimited, the arc voltage is definitely higher than within a cable. Therefore, in this investigation only tests with configurations of insulators for overhead lines and arcing fittings were performed.

In electric power supply networks the use of digital protection relays is growing. By means of microprocessors and distinct algorithms, these relays evaluate voltage and current vectors from the measured input signals and suppress effectively disturbing external effects, such as the superimposed arc voltage.

2 Power Arc Tests

For testing the above-mentioned protection algorithms power arc tests were performed in a high-power test laboratory. These tests were performed on original arrangements of insulators for overhead lines with arcing fittings for 20-kV, 110-kV and 220-kV lines. In these tests the input signals relevant to the distance protection, the line voltage and the line current, and in addition the arc voltage were measured (voltages by fast capacitive dividers, current by shunt or Rogowski coil), and they were digitized by a transient recorder of high resolution (12 bit) and high sampling rate (6 ms).

As the main task of this investigation, all the digitized variables were stored on magneto-optical discs and are thus available for developing or testing distance protection algorithms. In addition, using the recorded arc voltages and currents of various configurations of insulators tested, numerical fault arc models can be developed. With these models, transient input signals required for the distance protection can be calculated numerically for any configuration of the electric power system. Furthermore, using these calculated signals the distance protection algorithms can be developed or tested.

3 Test Arrangements and Test Circuits

With the 20-kV arrangement 102 power arc tests were performed. Two configurations of the insulator with the arcing horns (one solid-core insulator, horn distance 0.17 m) were tested, namely the suspension insulator (vertical arrangement) and the tension insulator (nearly horizontal arrangement). Simulated was a overhead line of 95/15 mm^2 ACSR with three different lengths corresponding to the prospective short-circuit currents (rms values) of I_{sc} = 2.0 kA, 3.2 kA and 5.5 kA.

With the 110-kV arrangement 115 power arc tests were performed in the vertical and the horizontal position of the insulator (one long rod insulator, ring distance 1.0 m). Simulated were single circuit lines 120/20 mm^2 and 240/40 mm^2 ACSR with four lengths corresponding to the prospective short-circuit currents (rms values) of I_{sc} = 5.0 kA to 12.5 kA in 2.5 kA steps. Also double cir-

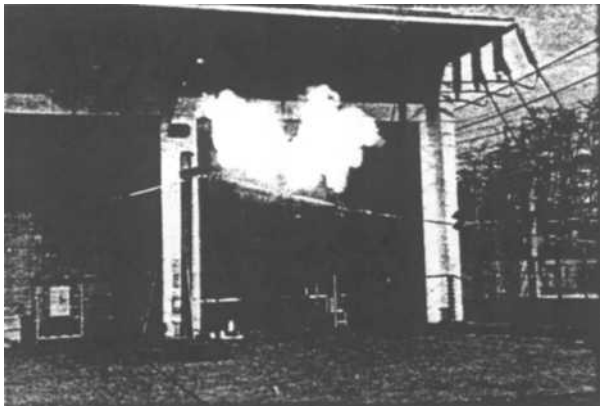

Fig. 1. Power arc test with the 220-kV arrangement in tension position (I_{sc} = 7.5 kA); double exposure

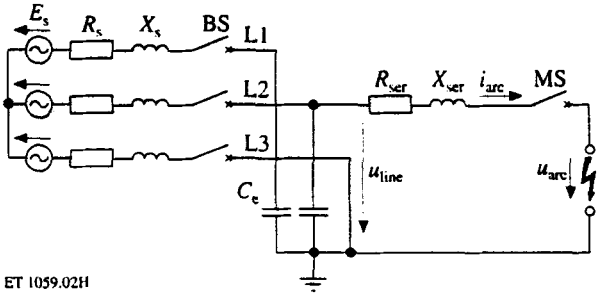

Fig. 2. Test circuit for power arc tests with insulators for overhead lines

$R_s + jX_s$	supply impedance	BS	breaking switch
$R_{ser} + jX_{ser}$	series line impedance	MS	making switch
C_e	line-to-earth capacitance		

cuit lines 120/20 mm² ACSR with different fault points in one circuit were simulated.

With the 220-kV arrangement 16 power arc tests were performed only in the horizontal position of the insulator (two long-rod insulators, ring distance 1.0 m each, total distance 2.5 m). Simulated was the same 240/40 line with the same short-circuit currents as in the 110-kV tests. **Fig. 1** shows a power arc test with the 220-kV arrangement and I_{sc} = 7.5 kA.

The test circuit shown in **Fig. 2** comprises all essential components to reproduce the distance protection input signals and the arc voltage as realistically as required. With the 20-kV and the 110-kV test circuits double earth faults were simulated, with the 220-kV test circuit single-phase short circuits were simulated. The supply circuits were represented with their short-circuit power and their capacitive earth fault current. By these means the relatively slow transients, induced by a short circuit, were realized. The overhead lines were represented only with their lead and return series impedance of the faulty phase. The relatively fast transients deriving from the line were not realized, but they are not relevant to the digital distance protection with its relatively low sampling frequencies of 2 kHz for instance.

The tests with the 20-kV arrangements were performed with full supply voltage, the network was represented with scale 1 : 1. In view of the required high power, the tests with the 110-kV and 220-kV arrangement could not be performed with full supply voltage. The supply voltage can be reduced as long as the short-circuit current maintains its sinusoidal waveform, i. e. is not influenced by the arc voltage. In the case of the intended longest horn distance of 2.5 m and the highest short-circuit current of 12.5 kA, the required sinusoidal current can be obtained with 20-kV supply voltage. Network elements, reactances, resistances and capacitances must be converted with the respective scale: for the double earth fault at 110 kV, the scale is 20 : 110 = 1 : 5.5, for the single-phase short-circuit at 220 kV, the scale is $20 : 220/\sqrt{3} = 1 : 6.35$.

Although the model reproduces the short-circuit current and the arc voltage quite realistically, the line voltage of the distance protection can be only approximately reproduced. In this case the line voltage can be calculated by means of a transient program with an implemented arc model as shown in the second part of this paper.

4 Arc Voltage During Arcing Time

The evaluation of the arc voltage peak in each half-period shows the movement of the arc during the arcing time of 290 ms. **Tab. 1** shows the measured arc voltages at arc initiation and the highest voltages that occurred during the arcing time for all arrangements tested. Oscillograms of some power arc tests are shown in chapter 6.

4.1 The 20-kV Arrangement

At arc initiation, i. e. immediately after melting and evaporation of the fusible wire, the arc voltage starts with values of 0.5 kV ... 0.75 kV and increases in the first instance to values near 2 kV. In tests with the low short-circuit current (2.0 kA) the arc voltage generally maintains this value. The higher currents (3.2 kA and especially 5.5 kA) cause the arc to elongate due to the higher electrodynamical force and the thermal buoyancy.

Insulator position	Test arrangement					
	20 kV		110 kV		220 kV	
	Arc initiation in kV	Maximum in kV	Arc initiation in kV	Maximum in kV	Arc initiation in kV	Maximum in kV
Suspension insulator	0.5 ... 0.75	6.0	0.8 ... 1.4	9.5	2.3 ... 3.4	no tests
Tension insulator		2.0		6.0		9.0

Tab. 1. Arc voltage of the three investigated test arrangements immediately after arc initiation and highest measured value during the arcing time of 290 ms for the suspension and the tension insulator

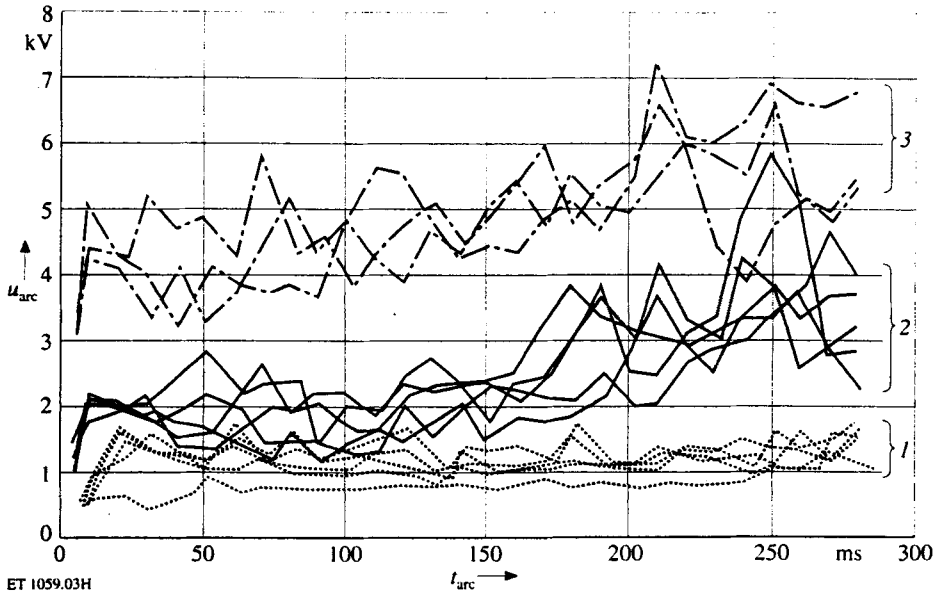

Fig. 3. Maximum arc voltage of each half-period during the arcing time; insulator in the tension position and I_{sc} = 5.5 kA
1 five tests with the 20-kV arrangement
2 six tests with the 110-kV arrangement
3 three tests with the 220-kV arrangement

For the three tested arrangements of insulators in the tension position and for a short-circuit current of 5.5 kA, **Fig. 3** shows for each case the maximum arc voltage of each half-period during the arcing time of 290 ms. For each arrangement, this figure indicates clearly the characteristic voltage range at arc initiation. Also, during the entire arcing time the arc voltage remains in a range which is characteristic for each arrangement, although temporary overlaps of adjacent ranges are possible.

Fig. 4 shows the maximum voltage of each half-period for the 20-kV arrangement (I_{sc} = 5 kA) and for the 110-kV arrangement (I_{sc} = 12 kA), both in the suspension position. In both arrangements the arc voltage at arc initiation is in the same range as in the tension position. In the further course of arcing time, in eight out of ten tests with the 20-kV arrangement, and in all seven tests with the 110-kV arrangement, the arc voltages rise steadily and, for both arrangements, have the same voltage values in the time interval from about 100 ms to 250 ms. Coincidentally, in this time interval abrupt voltage breakdowns occur on the arcs with the 20-kV arrangement, so that at the end of arcing time in all ten tests the arc voltage has again values below 2 kV. With the 110-kV arrangement the arc voltage also shows breakdowns but they are less severe.

Therefore the arc voltage time function depends in principle on the position of the insulators:

- In the *suspension position* of the insulator, the upper arcing horn is directed downwards to the line conductor. Therefore the arc can move with its lower root along the line conductor, the arc voltage can rise up to values of 6 kV, but if the arc root jumps back to the horn, the arc voltage diminishes to values below 2 kV.
- In contrast to the suspension position, in the *tension position* the insulator is rotated by 90°. Therefore a movement of the corresponding arc root along the line conductor is impossible. Consequently the arc burns steadily between the arcing horns, the arc voltage remains at values below 2 kV even at higher currents.

4.2 The 110-kV Arrangement

At arc initiation the arc voltage starts with values of 0.8 kV ... 1.4 kV. During the arcing time, in the suspension position the arc voltage rises to values up to 9.5 kV, especially at the higher currents (10.0 kA and 12.5 kA).

Because of the considerably large horn distance in comparison to the 20-kV arrangement, the arc elongates also in the tension position. Maximum values up to 6 kV were measured.

4.3 The 220-kV Arrangement

With the 220-kV arrangement only tests in the tension position were carried out. At arc initiation the arc voltage starts with values of 2.3 kV ... 3.4 kV. Because of the large horn distance in comparison to the 110-kV arrangement, the arc voltage rises to values up to 9 kV during the arcing time.

5 Numerical Arc Simulation

The goal of developing a fault arc model is to reproduce the dynamic interaction between the arc and the power system during a short-circuit through air with an acceptable accuracy. Once a general arc model is established and its parameters are determined for various insulator arrangements, digital simulation of transients can substitute for the demanding power arc tests. The signals produced numerically can be used to test and improve distance protection algorithms implemented in the digital protective relays for desired configurations of power networks.

5.1 Dynamic Arc Model

Based on the prior work [5] of the same author, the dynamic fault arc model has been improved to take the random behaviour of the arc into consideration. The arc parameters are obtained automatically by numerical analysis of the time functions of arc current and arc voltage.

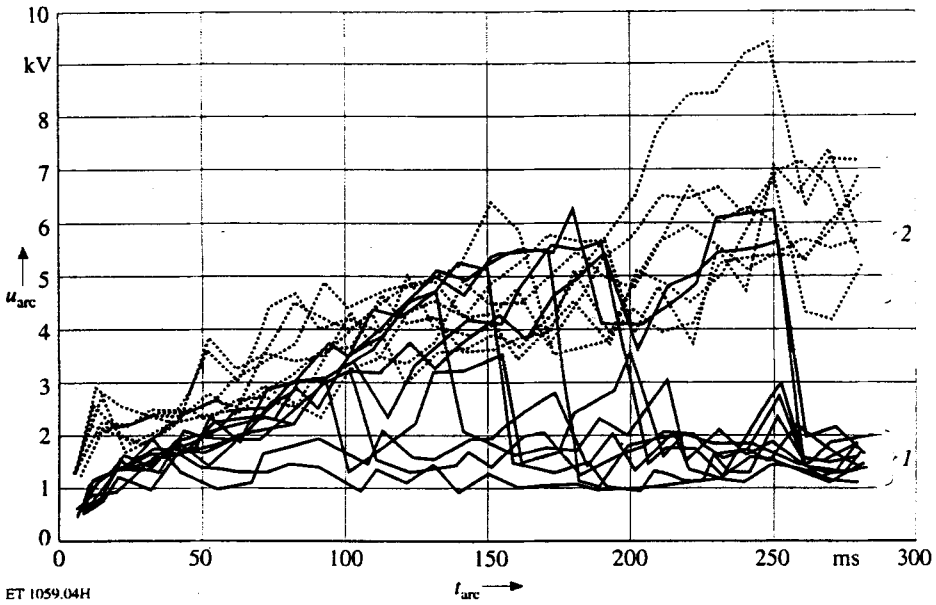

Fig. 4. Maximum arc voltage of each half-period during the arcing time; insulator in the suspension position
1 ten tests with the 20-kV arrangement and $I_{sc} = 5.5$ kA
2 seven tests with the 110-kV arrangement and $I_{sc} = 12.5$ kA

i_{arc} instantaneous arc current,
l_{arc} time-varying arc length.

The stationary arc conductance follows as:

$$G = \frac{|i_{arc}|}{u_{st}}. \tag{3}$$

The current-dependent portion of the stationary arc voltage can be attributed physically to the partial time-varying arc elongation in each half-period because of the magnetic force due to the short-circuit current. It influences the arc behaviour significantly for long arcs (110-kV and 220-kV insulator arrangements) as will be shown later.

As explained in [5], the dynamic behaviour of the fault arc through air is described by the power balance relation between the electric input power and the heat dissipation to the surrounding air. Based on the theory of black box models of the switching arc [6], it is assumed that the arc channel is at a constant temperature, which is independent of the arc current. An increase of the energy of the arc column causes an increase of the cross-section of the arc. Whereas the stationary electric field strength is supposed to be constant, the stationary arc voltage varies with the continuously changing arc length. These assumptions allow to describe the electric arc by a first order differential equation, where the arc conductance is expressed as a function of the heat content of the arc column. The arc equation of *Hochrainer* [7] is used to describe the dynamic behaviour of a fault arc through air:

$$\frac{dg}{dt} = \frac{1}{\tau}(G - g) \tag{1}$$

where

g instantaneous arc conductance,
G stationary arc conductance,
τ arc time constant.

Deviating from the switching arc black box models, the stationary arc voltage is assumed to be not constant for fault arcs burning in air freely, but it depends on the arc length and partly on the short-circuit current flowing through the arc. It is expressed as follows

$$u_{st} = (u'_0 + r'_0 |i_{arc}|)\, l_{arc} \tag{2}$$

where

u_{st} stationary arc voltage,
u'_0 characteristic arc voltage per arc length,
r'_0 characteristic arc resistance per arc length,

5.2 Determination of Arc Parameters

The basic arc parameters u_0, r_0 and τ are determined by means of computer programs automatically using the digitally recorded time functions of arc current and arc voltage. The instantaneous arc conductance is computed additionally from the arc current and arc voltage using the relation

$$g = \frac{i_{arc}}{u_{arc}} \tag{4}$$

based on the assumption that the arc has purely resistive characteristics.

A numerical method that involves the integration of the measured time functions has to be preferred to determine the arc parameters u_0, r_0 and τ, since the arc shows rather random behaviour depending on the surrounding conditions, such as wind velocity, buoyancy, vertical or horizontal position of insulators, etc.

It is assumed that the arc parameters are constant during a half-period of arc current and voltage. First the unknown parameters u_0 and r_0 are determined by solving the following two linear eqs. (5) and (6), which are derived from eq. (1) by integration with the limits as indicated in **Fig. 5** for the arc conductance:

$$u_0 \int_{t_1}^{t_5} \frac{1}{|u_{arc}|}\, dt + r_0 \int_{t_1}^{t_5} g\, dt = t_5 - t_1\,; \tag{5}$$

$$u_0 \int_{t_2}^{t_4} \frac{1}{|u_{arc}|}\, dt + r_0 \int_{t_2}^{t_4} g\, dt = t_4 - t_2\,. \tag{6}$$

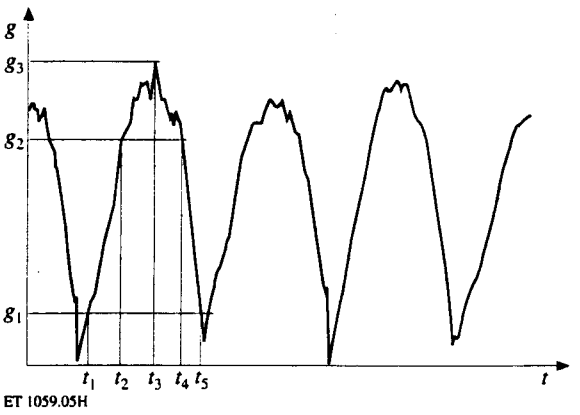

Fig. 5. Integration limits in a half-period of the arc conductance

Eqs. (5) and (6) are approximate in the sense that the integral of G/τ within the stated limits is assumed to be constant.

The arc time constant τ is calculated with the known u_0 and r_0 through integration in the time intervals either from t_1 to t_3 or from t_3 to t_5

$$\tau = \frac{\int_{t_1}^{t_3} G\,dt - \int_{t_1}^{t_3} g\,dt}{g_3 - g_1}. \qquad (7)$$

The trapezoidal rule of integration is used to compute the integrals in eqs. (5) to (7). This method is repeated successively for a sequence of half-periods in the time interval selected, where no significant elongation of the arc can be observed visually from the time function of the arc voltage. This way the basic arc parameters can be obtained, which are representative for each insulator arrangement of voltage levels 20 kV, 110 kV and 220 kV.

As given in **Fig. 6** and **7** for all insulator arrangements tested, the stationary arc characteristics (u_{st} versus i_{arc}) and arc time constant τ obtained by evaluation of the measurements scatter in a wide range (shaded area in Fig. 6) depending on the time-varying, random behaviour of the arc. The physically non-realistic values of arc parameters due to the high distortion of waveforms of arc voltages as a result of rush elongation and partial breakdown of the arc were eliminated. In Fig. 6 the intercept on the y-axis gives u_0 and r_0 represents the slope of the lines. The lines drawn in Fig. 6 indicate the mean regression curves belonging to the arc tests carried out for various prospective short-circuit currents stated in chapter 3.

The characteristic arc resistance r_0 cannot be determined reliably from the measurements of the 20-kV arc tests, because of the relatively small value of the resistance, which is drowned by the random behaviour of the arc. For this reason, the 20-kV arc measurements were evaluated using a simplified formula with the assumption of $r_0 = 0$. Fig. 6a and 6b show therefore ranges of a constant stationary arc voltage for the 20-kV arc tests.

The range of the variation of the arc time constant in Fig. 7 is indicated by error bars, where the markers point

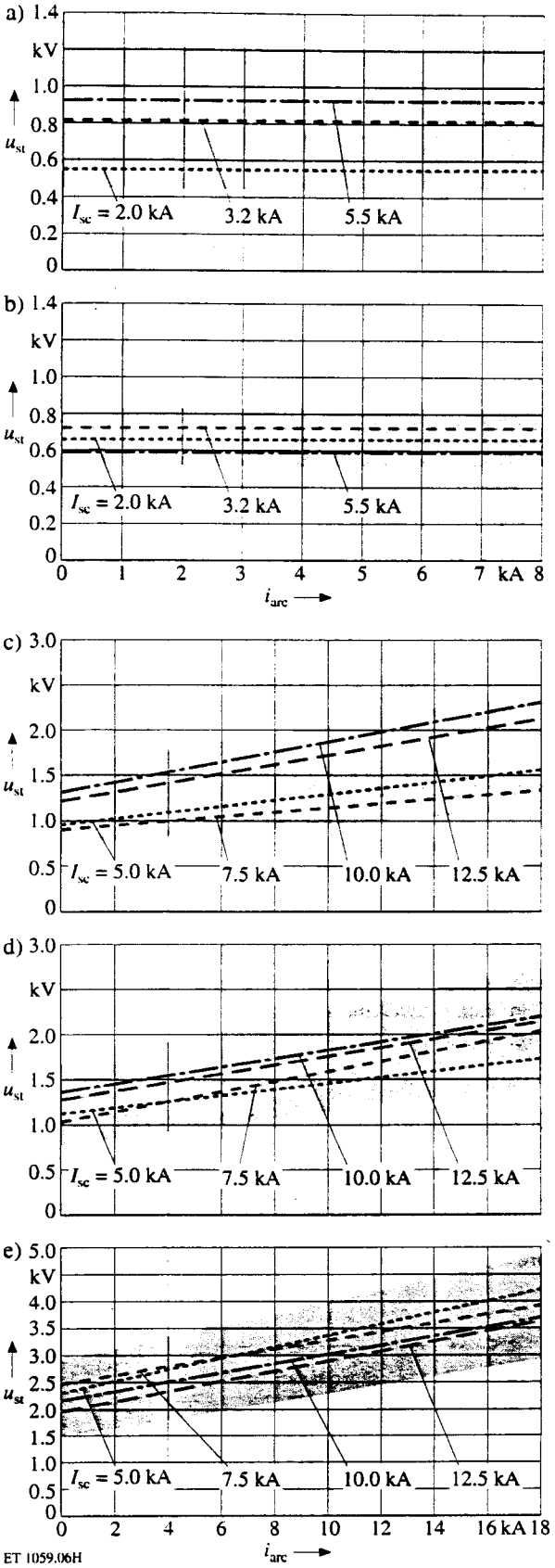

Fig. 6. Stationary arc characteristics
a) 20-kV insulator arrangement in suspension position
b) 20-kV insulator arrangement in tension position
c) 110-kV insulator arrangement in suspension position
d) 110-kV insulator arrangement in tension position
e) 220-kV insulator arrangement in suspension position

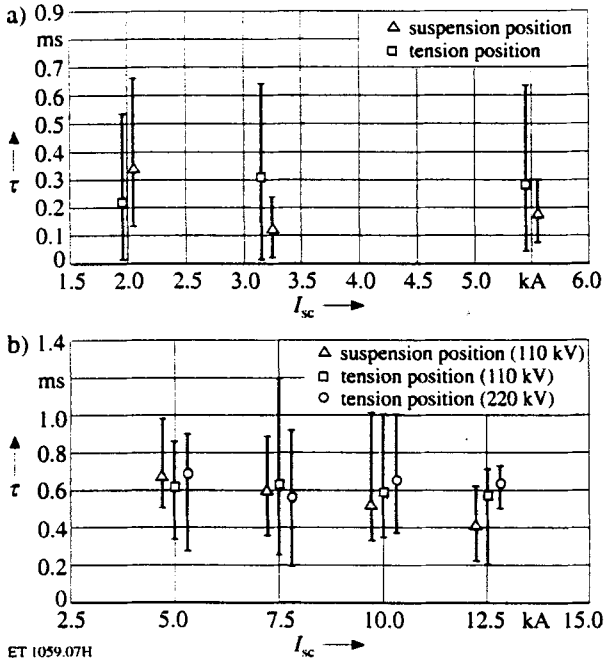

Fig. 7. Arc time constant obtained from arc tests with different short-circuit currents
a) 20-kV insulator arrangement
b) 110-kV and 220-kV insulator arrangement

to the mean values. Whereas the 20-kV arcs possess relatively small time constants, which is an indication of a brisk arc behaviour, the time constants of the 110-kV and 220-kV arcs vary in the same range.

In **Fig. 8** the mean values of the characteristic arc parameters u_0 and r_0 are plotted as a function of the horn distance for the horizontal position of insulators. The values for the 20-kV arcs were calculated by extrapolation using constant stationary arc voltages given in Fig. 6a and 6b.

5.3 Arc Simulation in the ATP-EMTP

Digital simulations of the power arc tests were performed using the royalty-free universal transients program ATP-EMTP [8]. The dynamics of the electric arc including the random behaviour of the arc parameters u_0, r_0, τ and the arc length l are represented using MODELS [9], which is a general-purpose simulation language interfaced to the ATP-EMTP. The dynamic interaction between the electric circuit and MODELS for the simulation of a fault arc as a time-varying resistance is very similar to what has been sufficiently described in [6] and [9].

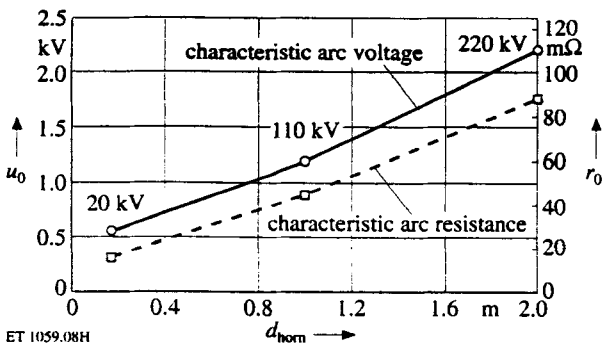

Fig. 8. Mean value of arc parameters u_0 and r_0 determined from the arc tests with the horizontal insulation arrangement as a function of the horn distance d_{horn}

The arc eq. (1) including the expressions for u_{st} and G given in eqs. (2) and (3) is solved at each time step using the library function Laplace of MODELS [9] through the equation:

$$g(t) = \frac{1}{1+\tau s} G(t) \tag{8}$$

where τ does not need to be a constant coefficient.

The random behaviour of the arc length, which influences the stationary arc voltage u_{st} according to eq. (2), is realized in MODELS through a sophisticated algorithm, which was developed by analysing the arc measurements. The length variation of the arc simulated using MODELS in the first numerical example is given in section 6.1.

The variation of the arc parameters u_0, r_0 and τ during arcing time within the range given in Fig. 6 and 7 is considered by a random signal, which is filtered using a third-order, low-pass Butterworth filter with the corner frequency of 100 Hz in order to create slowly varying arc parameters.

6 Comparison of Test and Simulation Results

6.1 The 20-kV Insulator Arrangement

Two power arc tests were selected to compare the test and simulation results. The measured time functions of the selected 20-kV arc test with a vertical insulator arrangement and a prospective short-circuit current (rms value) of $I_{sc} = 5.5$ kA are given in **Fig. 9a** to **9c**. The arc parameters obtained by evaluating the half-periods according to the method given in section 5.2 are shown in **Fig. 9d** to **9e**. As it can be deduced from Fig. 9c and 9d, the arc elongates steadily starting from $t = 100$ ms until $t = 200$ ms and after reaching approximately five times of its initial length, it breaks down abruptly to the initial length.

The simulation results of the same case with the basic arc parameters determined from the measurements are given in **Fig. 10**. The test circuit given in Fig. 2 was modelled in the ATP-EMTP by lumped *RLC*-circuit elements. The 20-kV power source is represented by its no-load voltage and short-circuit impedance. Since the neutral point was isolated, the equivalent line-to-earth capacitance was also modelled in the test circuit. The series impedance representing the transmission line is chosen such that the prospective short-circuit current (rms value) $I_{sc} = 5.5$ kA flows through the circuit. The electrical data of the test circuit are given as follows:

$E_s = 20\ \text{kV}/\sqrt{3}$ (rms value),

$Z_s = R_s + \text{j}\,X_s = (0.05 + \text{j}0.92)\ \Omega$ (corresponding to $S''_k = 435$ MVA),

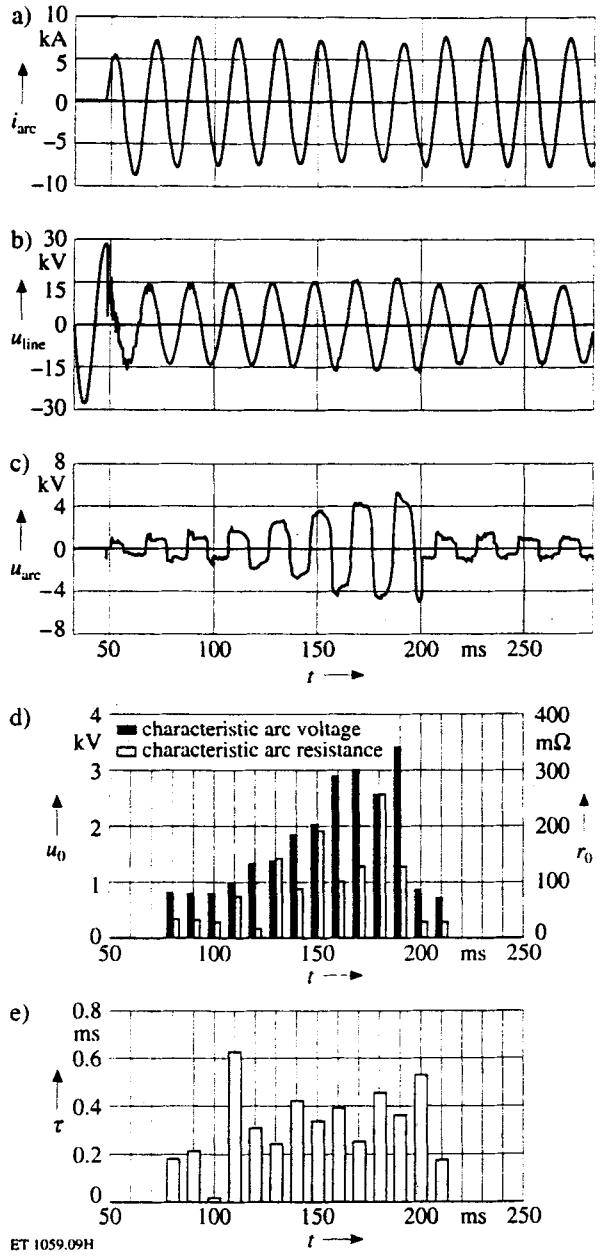

Fig. 9. Power arc test with the vertical 20-kV insulator arrangement (I_{sc} = 5.5 kA)
a) measured arc current
b) measured line voltage
c) measured arc voltage
d) calculated arc parameters u_0 and r_0
e) calculated arc time constant

$C_e = 13.7\ \mu F$,

$Z_{ser} = R_{ser} + j X_{ser} = (0.82 + j\,1.50)\ \Omega$.

An additional resistance of 80 Ω is connected parallel to the supply reactance in the numerical model of the circuit in order to reproduce the actual damping of the test circuit.

Besides the computed time functions of arc current, arc voltage and line voltage, the arc length variation with a superimposed random signal and time variation of the arc parameters u_0 and r_0 according to a random signal are shown in Fig. 10d to 10f.

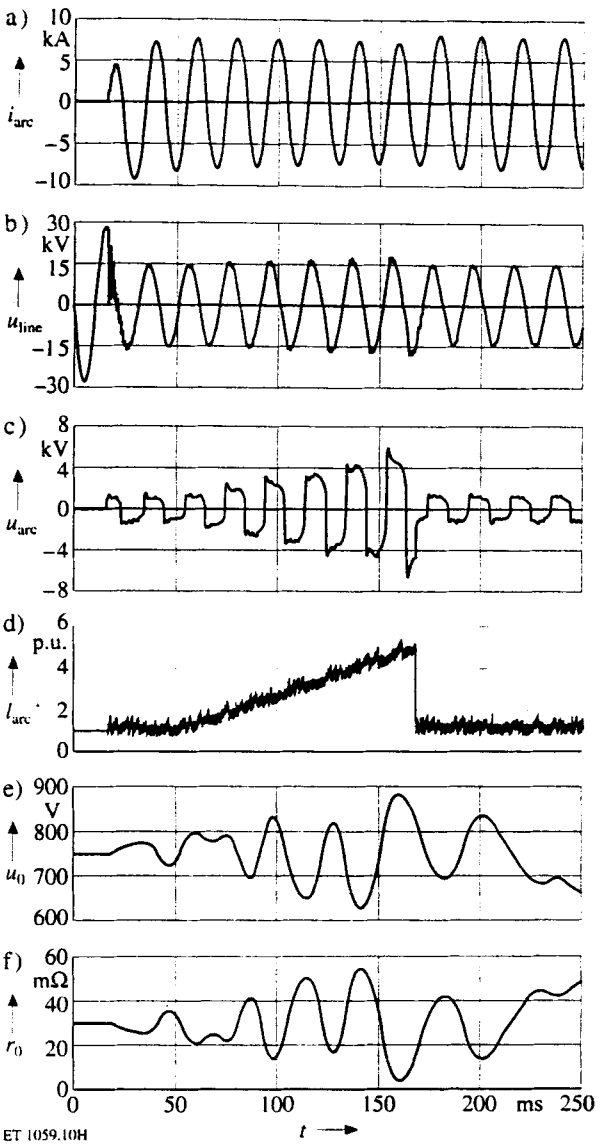

Fig. 10. Numerical simulation of the power arc test with the 20-kV insulator
a) arc current
b) line voltage
c) arc voltage
d) arc length variation
e) random variation of u_0
f) random variation of r_0

6.2 The 110-kV Insulator Arrangement

This power arc test with a 110-kV insulator arrangement is used to show the impact of the fault arc on the line voltage of the equivalent real 110-kV network. This selected arc test was performed in the vertical position of the 110-kV overhead line insulator with the series impedance of the modelled single circuit overhead line 120/20 mm² ACSR corresponding the short-circuit current (rms value) of 12.5 kA. The electrical data of the test circuit given in Fig. 2 are given as follows

$E_s = 20.1\ kV/\sqrt{3}$ (rms values),

$Z_s = R_s + jX_s = (0.04 + j0.67)\ \Omega$ (corresponding to $S''_k = 600$ MVA),

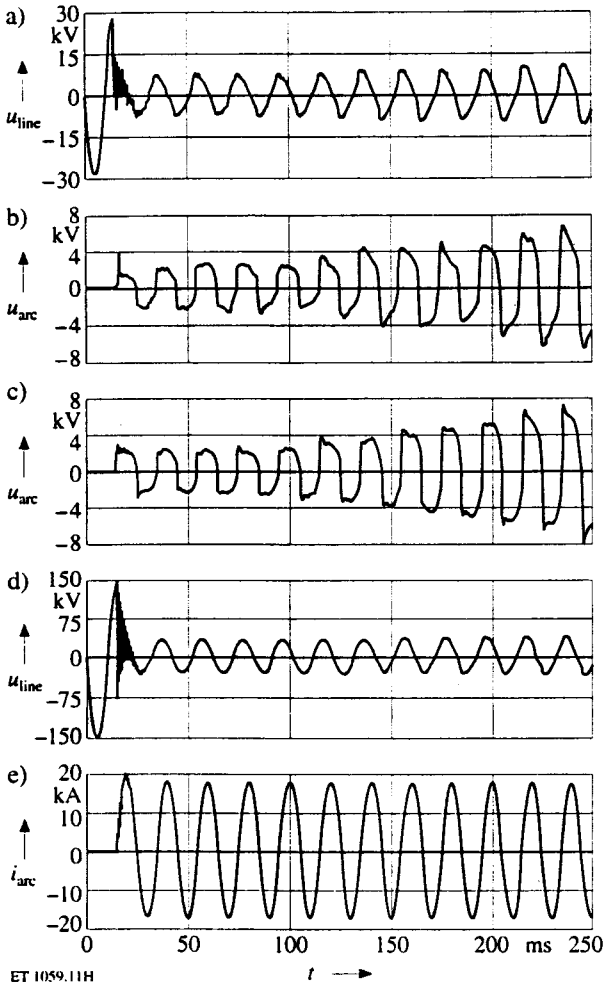

Fig. 11. Power arc test with the vertical 110-kV insulator arrangement (I_{sc} = 12.5 kA)
a) measured line voltage
b) measured arc voltage
c) simulated arc voltage (110-kV network model)
d) simulated line voltage (110-kV network model)
e) simulated arc current (110-kV network model)

$C_e = 27.4\ \mu F$,

$Z_{ser} = R_{ser} + j X_{ser} = (0.117 + j 0.260)\ \Omega$.

In order to simulate the equivalent 110-kV power network with the same short-circuit current all the impedances and the source voltage must be multiplied by the scaling factor 5.5 as explained in chapter 3. **Fig. 11** shows the measured line voltage and the arc voltage of the 20-kV test circuit as well as the computed voltages and currents of the equivalent 110-kV network. It can be noticed that the distortion of the line voltage of the 110-kV network (Fig. 11d) due to fault arc is significantly lower than of the measured line voltage in the 20-kV test circuit (Fig. 11a).

7 Conclusions

Extensive power arc tests were carried out with the original arrangements of overhead line insulators and arcing fittings of nominal voltage levels 20 kV, 110 kV and 220 kV. A test circuit with a 20-kV power source was modelled to achieve prospective short-circuit currents in the range of 2 kA to 12.5 kA (rms values). Arc tests have been performed in the horizontal and vertical position of the insulators.

During the tests the input signals relevant to the distance protection, line voltage and line current as well as the arc voltage were measured. They were digitized by a transient recorder of high resolution and high sampling rate. The discrete measured data were stored on magneto-optical discs and are thus available for developing or testing distance protection algorithms.

Using the recorded arc voltages and currents of various configurations of insulators tested, an existing numerical arc model has been improved to take the random behaviour of the arc into consideration. The arc parameters were determined by numerical analysis of recorded time functions. A general arc model has been established, which allows the digital simulation of arcs of various insulator arrangements.

The numerical simulation of the selected two cases shows a good agreement between the measured and computed time functions. The numerical arc model is realized in the universal electromagnetic transients program ATP-EMTP, which allows the representation of any network configuration to be investigated, so the digital simulation of arc faults through air can substitute for demanding power arc tests. The signals produced by ATP-EMTP can be used to test and improve distance protection algorithms implemented in the modern digital protective relays.

8 List of Symbols and Abbreviations

8.1 Symbols

C_e	line-to-earth capacitance
E_s	source voltage
g	instantaneous arc conductance
G	stationary arc conductance
i_{arc}	arc current
I_{sc}	prospective short-circuit current
l	arc length
r_0	characteristic arc resistance
R_s	equivalent source resistance
R_{ser}	series line resistance
s	Laplace operator
S''_k	initial symmetrical short-circuit power
t	time
u_{arc}	arc voltage
u_{line}	line-to-earth voltage
u_{st}	stationary arc voltage
u_0	characteristic arc voltage
X_s	equivalent source reactance
X_{ser}	series line reactance
τ	arc time constant

8.2 Abbreviations

ATP-EMTP	Alternative Transients Program - Electromagnetic Transients Program
ACSR	Steel Reinforced Aluminium Conductor

References

[1] IEC 36B (Sec.) 116 (Draft): Insulators for Overhead Lines with a Nominal Voltage above 1000 V, A.C. Power Arc Tests on Insulator Sets. Frankfurt a. M./Germany: Germ. Electrotech. Commiss. (DKE), 1993

[2] *Nelles, D.; Opperskalski, H.:* Digitaler Distanzschutz: Verhalten der Algorithmen bei nicht idealen Eingangssignalen. Wiesbaden/Germany: Dt. Univ.-Verl., 1991

[3] *Opperskalski, H.:* Verhalten impedanzbestimmender Distanzschutzalgorithmen. Düsseldorf/Germany: VDI, 1991 (Fortschr.-Ber. R. 6, no. 256)

[4] *Nilges, J.:* Die Anwendung des Distanzschutzprinzips zur Kurzschlußerfassung auf Drehstrom-Doppelleitungen. Düsseldorf/Germany: VDI, 1990 (Fortschr.-Ber. R. 21, no. 73)

[5] *Kizilcay, M.; Pniok, T.:* Digital Simulation of Fault Arcs in Power Systems. ETEP Eur. Trans. on Electr. Power Engng. 1 (1991) no. 1, pp. 55–60

[6] CIGRE Working Group 13.01: Practical application of arc physics in circuit breakers. Survey of calculation methods and application guide. Electra No. 118, 1988, pp. 65–79

[7] *Hochrainer, A.:* Eine regelungstechnische Betrachtung des elektrischen Lichtbogens, kybernetische Theorie des Lichtbogens. ETZ-A Elektrotech. Z. 92 (1971) no. 6, pp. 367–371

[8] Alternative Transients Program – Rule Book. Portland, Oregon/USA: Canadian/American EMTP User Group. 1992

[9] *Dubé, L.; Bonfanti, I.:* MODELS: A New Simulation Tool in the EMTP. ETEP Eur. Trans. on Electr. Power Engng. 2 (1992) no. 1, pp. 45–50

Acknowledgment

The authors would like to acknowledge the Ministry for Economic Affairs of the Federal Republic of Germany for financial assistance of the AiF-project 8507.

Manuscript received on November 16, 1993

The Authors

Dr.-Ing. Mustafa Kizilcay (1955), VDE, received the B.S. degree in electrical engineering from Middle East Technical University in Ankara/Turkey in 1979. That same year, he joined the Turkish Electricity Authority (TEK) in Ankara as a research engineer. In 1985, he received the Dipl.-Ing. degree in electrical engineering from the University of Hannover/Germany. From 1985 to 1990, he was a member of the scientific staff of "Institut für Elektrische Energieversorgung" of the University of Hannover. After a short period with AEG's Dept. of Protective Relay Development in Frankfurt/M, Germany, early in 1991, he moved to his present position with Lahmeyer International GmbH in Frankfurt/M where, as a consulting engineer, he has responsibility for power system studies. In 1991, he was awarded his doctorate in electrical engineering from the University of Hannover. He was a contributor to EMTP development through the Leuven EMTP Center in Leuven/Belgium, where he was a faculty member of the 1989, 1991 and 1993 EMTP short courses. (Lahmeyer International, RE 2, Lyoner Str. 22, D-60528 Frankfurt/M, T +49 69/66 77-2 54, Fax +49 69/66 77-3 22)

Karl-Heinrich Koch (1942) received the Dipl.-Ing. degree in Electrical Engineering from the Technical University of Darmstadt/Germany. Afterwards he joined the high power laboratory of FGH in Mannheim/Germany as a Research Engineer. His fields of interest are the transient performance of current transformers, the extinction of earth-fault current by compensation and power-system studies with the EMTP. (Forschungsgemeinschaft für Hochspannungs- und Hochstromtechnik e.V., Hallenweg 40, D-68219 Mannheim, T +49 621/804 72 60, Fax +49 621/804 72 59)